

## THE INFLUENCE OF SOME POWDERS ON THE ANTIMICROBIAL ACTIVITY OF PLA PACKAGING WITH OREGANO OIL ADDITIVES

Andreea Cătălina JOE<sup>a</sup>, Ion ONUȚU<sup>a\*</sup>,  
Dorin BOMBOȘ<sup>a,f</sup>, Gabriel VASILIEVICI<sup>b</sup>, Abeer BAIOUN<sup>c</sup>,  
Laura SILAGHI-DUMITRESCU<sup>d</sup>, Ioan PETEAN<sup>d,e</sup>

**ABSTRACT.** This study investigates the antimicrobial potential and physicochemical performance of PLA-based biocomposite films incorporated with bioglass, oregano essential oil, and diacetin as a green plasticizer. Designed for use in food packaging applications, the films aim to serve as biodegradable, active barriers against microbial contamination while ensuring environmental compatibility and material safety. Initial microbiological screening identified the PB2 formulation comprising 70% PLA, 25% diacetin, 3% bioglass, and 2% oregano oil as the most effective antimicrobial composition. PB2 achieved a 79% inhibition of bacterial growth after two days and maintained 65% suppression after 14 days, confirming its long-term antimicrobial efficacy. To gain a comprehensive understanding of PB2's behavior, extensive characterization was performed. FTIR spectroscopy confirmed the successful incorporation of functional groups from both PLA and active additives. TGA and DSC analyses revealed enhanced thermal stability and a delayed glass transition ( $T_g > 83$  °C), attributed to the stiffening effect of bioglass. SEM and AFM investigations demonstrated uniform nanoparticle dispersion and low

<sup>a</sup> Department of Petroleum Refining Engineering and Environmental Protection, Petroleum-Gas University of Ploiesti, 39 Bucharest Blvd., 100680 Ploiesti, Romania

<sup>b</sup> National Institute for Research Development for Chemistry and Petrochemistry-ICECHIM-București, 202 Spl. Independenței, 060021 Bucharest, Romania

<sup>c</sup> Chemistry Department, Faculty of Science, University of Damascus, Damascus, Syria

<sup>d</sup> Babes-Bolyai University, "Raluca Ripan" Institute for Research in Chemistry, 30 Fântânele Str., 400294 Cluj-Napoca, Romania

<sup>e</sup> Faculty of Chemistry and Chemical Engineering, Babes-Bolyai University, 11 Arany János Str., 400028 Cluj-Napoca, Romania

<sup>f</sup> S.C. Medacril S.R.L., 8 Carpați Street, 551022 Mediaș, Romania

\* Corresponding author: ionutu@upg-ploiesti.ro



surface roughness ( $R_a=30.1$  nm), ensuring good structural homogeneity. Mechanical testing showed reduced tensile strength but significantly increased elongation at break, indicating greater ductility due to matrix amorphization promoted by diacetin. Altogether, the results support the potential of PB2 as a multifunctional, antimicrobial biocomposite film suitable for food-grade and biomedical applications.

**Keywords:** *diacetin, oregano oil, bioglass, antimicrobial barrier, active food packaging*

## INTRODUCTION

Driven by the increasing urgency of climate change, the European Union has implemented strategies aimed at reducing environmental pollution by encouraging recycling, minimizing the consumption of conventional plastic materials, and replacing them with biodegradable alternatives. These policies not only address sustainability concerns but also promote public health [1]. A major challenge lies in the insufficient infrastructure for the collection, sorting, and recycling of plastic waste. Moreover, accidental incineration of such materials continues to undermine the enforcement of EU Directive 2019/909 [2].

Within this context, the role of food packaging has gained increasing attention, particularly in light of microbial risks associated with surface contamination [3,4]. Ensuring food safety requires controlling microbial growth and mitigating environmentally driven pathogenic risks caused by pollution and improper waste management practices [5,6]. One promising approach involves the development of bioactive packaging that can act as a functional barrier against microbial colonization and proliferation [7-9].

Oregano essential oil has shown potent antifungal activity, effectively inhibiting the growth of hyphae, spores, filamentous fungi, and molds [10-12]. It is also important to consider how solvents affect membrane properties, especially in terms of selectivity and mechanical strength [13]. In this regard, polylactic acid (PLA) has emerged as a suitable biodegradable polymer offering both structural stability and environmental compatibility [14,15].

The shift from petrochemical plastics and toxic solvents traditionally used in membrane manufacturing toward sustainable, eco-friendly membrane technologies stems from the growing recognition of their reduced ecological footprint. Researchers have highlighted the need to adopt green solvents and biodegradable polymers, leading to a redefinition of membrane fabrication protocols aligned with environmental sustainability [16].

Most synthetic polymers used in food packaging are petroleum-based, raising significant ecological concerns and prompting global efforts to phase them out [17,18]. In contrast, biopolymer-based films such as those derived from PLA not only extend food shelf life but are also safe for direct food contact. Essential oils have emerged as natural alternatives to synthetic preservatives, offering both antimicrobial and antioxidant functionalities. Despite the European recycling rate of plastic standing at only 7%, global demand for plastic remains the third highest after steel and cement. Thus, the gradual shift toward biodegradable food packaging is accelerating. Notably, multilayered systems combining polar and nonpolar biodegradable polymers have demonstrated efficacy in limiting gas exchange between packaged food and the surrounding atmosphere [19].

The effectiveness of active packaging films is governed by multiple factors, including the type of structural biopolymer used, the nature and dosage of active compounds, the retention and release kinetics of these agents, storage conditions, and the specific microbial strains tested. Studies have shown that oregano essential oil can be successfully dispersed in biocomposite matrices such as carboxymethyl cellulose (CMC) and agar without inducing surface defects like pores or cracks [9]. This phenomenon has been attributed to the enhanced compatibility between the essential oil and the biopolymer network. Although PLA is inherently brittle, its functionality in this context was preserved. Diacetins were employed as green plasticizers to improve the flexibility and processability of PLA [8,20], while the antimicrobial efficacy of oregano oil vapors at low concentrations further justified their incorporation into packaging systems [21]. In animal feed applications, oregano oil has demonstrated antimicrobial action against *Escherichia coli* and *Salmonella*, further supporting its versatility as a functional additive [22,23].

Various *in vitro* assays have been developed to assess the antimicrobial performance of polymer matrices loaded with essential oils. The oil–matrix interaction may influence the diffusion of active agents into the surrounding environment, thus modulating antimicrobial efficiency. Commonly used methods include disc diffusion, agar well diffusion, and agar dilution techniques. Nanocomposite films incorporating essential oils such as clove, coriander, cumin, marjoram, cinnamon, and caraway have been shown to inhibit *E. coli*, *S. aureus*, and *L. monocytogenes* using agar diffusion protocols [9].

Over the past five decades, bioactive glass has emerged as a multifunctional material widely employed in medical fields, particularly for its antibacterial properties and applications in tissue engineering. When combined with natural polymers, it has proven effective in biological and biomedical contexts [24]. Studies indicate that gelatin–bioactive glass composites offer enhanced mechanical performance and biocompatibility. Reduced inflammatory

response has also been observed in glycerin bioglass systems. Moreover, lyophilized composites of chitosan and bioglass have shown potential in bone tissue engineering [1]. Bioactive glass continues to be regarded as a third-generation material for soft tissue regeneration although skin regeneration remains challenging due to the lack of a universally effective wound-healing formulation [24].

In this study, we aimed to develop a fully biodegradable packaging film composed of polylactic acid (PLA), an eco-friendly plasticizer (diacetins), and oregano essential oil. The antibacterial performance of the essential oil was evaluated under in situ release conditions, in the presence of various powders with distinct textures. Microbiological tests were conducted to assess the antimicrobial effectiveness of the developed formulations. Building upon this foundation, this manuscript presents a novel approach in the development of biodegradable active packaging films by integrating bioglass and oregano essential oil into a PLA matrix plasticized with diacetin. Unlike previous studies that focused solely on antimicrobial efficacy, this research offers a comprehensive characterization combining microbiological testing with advanced thermal, mechanical, and morphological analysis. The long-term antimicrobial stability and enhanced ductility of the PB2 formulation highlight its promising potential for both food-grade and biomedical applications, marking a significant advancement in the design of multifunctional biocomposite materials.

## RESULTS AND DISCUSSION

### Evolution of the inhibition zone on solid media

Following microbiological testing, the evaluation of microbial growth in the presence of PLA-based films with varying chemical compositions revealed that the PD3 formulation comprising 73.0% PLA, 25% diacetin, and 2.0% oregano essential oil exhibited the largest inhibition zones on both culture media types: MB (bacterial) and MA (algal) (Figure 1). These media were specifically designed to promote microbial proliferation, thus providing a robust environment for testing the films' antimicrobial efficacy.

The pronounced inhibition effect observed around PD3 samples suggests that the higher concentration of the active compound (oregano oil at 2.0%) successfully created a localized antimicrobial buffer zone, preventing the proliferation of *Bacillus subtilis* as well as the seeded *Chlorella* sp. culture on the Petri dishes.

THE INFLUENCE OF SOME POWDERS ON THE ANTIMICROBIAL ACTIVITY OF  
PLA PACKAGING WITH OREGANO OIL ADDITIVES

This clear suppression of cellular development near the PD3 film confirms the superior antimicrobial performance of this specific formulation. The results support the hypothesis that increasing the concentration of natural active agents in biodegradable films can significantly enhance their protective role, making them promising candidates for active food packaging applications.

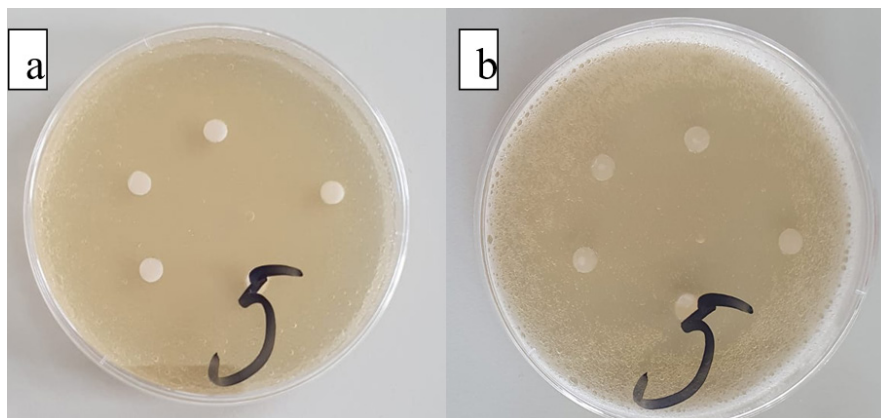


**Figure 1.** Presentation of the antimicrobial effect of sample PD3 in MB medium:  
(a) appearance of the culture medium on the second day of monitoring;  
(b) evolution of the antimicrobial effect of the PD3 film component  
on the 14th day of monitoring

Based on these promising results, six additional active film formulations were developed. Each of these samples contained 25% diacetin and 2.0% oregano oil, and were supplemented with one of three functional additives activated carbon, Aerosil, or Bioglass at two concentrations (2% and 3%). The detailed compositions of these six samples are summarized in Table 1, highlighting their potential for enhanced antimicrobial performance through synergistic effects between the matrix and active fillers.

To evaluate the antimicrobial inhibition potential of PLA films containing different functional additives alongside the reference sample PD3 a nutrient-rich liquid medium was prepared using the following composition: 0.5 g yeast extract, 7 g casein, 3 g glucose, 0.25 g L-cysteine, 1.25 g sodium chloride, and 0.25 g sodium thioglycolate, with distilled water added to a final volume of 500 mL [25].

The components were dissolved in a water bath at 60 °C for 15 minutes to ensure complete homogenization. After cooling the medium to 35 °C, 50 mL of a *Bacillus subtilis* suspension ( $10^{-4}$  cells/mL) was added. The resulting biological mixture was stirred at 200 rpm for 30 minutes to ensure uniform distribution of bacterial cells.

The medium was then distributed into eight sterile test tubes labeled I through VIII. Each tube contained 10 mL of the inoculated medium and was supplemented with two circular PLA discs (7 mm in diameter) from one of the following samples: PD3, PC1, PC2, PS1, PS2, PB1 and PB2. The eighth tube served as the control (blank), containing only the medium and bacterial suspension without any film sample.

All test tubes were incubated at 35 °C for 14 days under sterile conditions. Bacterial growth was monitored throughout the incubation period to assess the inhibitory effect of each formulation and compare their relative antimicrobial efficiencies.

### Optical density measurement (OD<sub>500</sub>)

Cell growth within the biological suspension was assessed spectrophotometrically by measuring the optical density at a wavelength of 500 nm (OD<sub>500</sub>). To monitor the dynamics of bacterial proliferation in the culture medium [26-29], daily measurements were performed over a 14-day incubation period.

For each measurement, a 1 mL aliquot was withdrawn from each test tube and analyzed using a UV-Vis spectrophotometer (model T85+, PG Instruments).

The optical density data revealed that the active compounds incorporated into the film samples functioned as effective bacterial growth inhibitors (Figure 2). Among all tested formulations, PB2 demonstrated the highest inhibitory performance: bacterial growth was suppressed by 79% relative to the blank after 2 days, and by 65% after 14 days. These findings highlight the long-term antimicrobial potential of Bioglass-based PLA films.

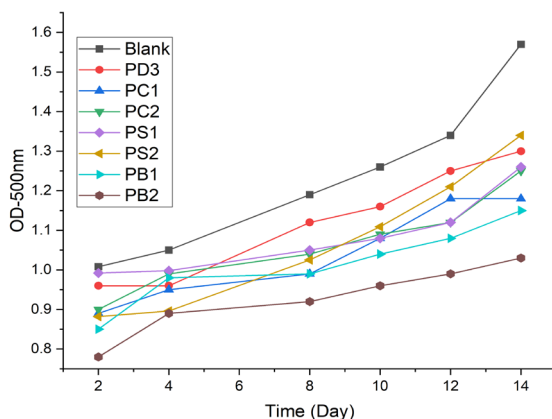


**Figure 2.** Optical Density Analysis of Samples PD3, PC1, PC2, PS1, PS2, PB1, and PB2 Over a 14-Day Period

Based on these promising results, the PB2 sample underwent comprehensive characterization using scanning electron microscopy (SEM), Fourier-transform infrared spectroscopy (FTIR), atomic force microscopy (AFM), thermal analysis (TGA and DSC), and tensile strength testing. These analyses aim to provide an integrated evaluation of the sample's microstructural, thermal, surface, and mechanical properties to support its suitability for biomedical and dermato-cosmetic applications.

### FT-IR analysis

The FTIR spectrum of PB2 sample presented in the figure 3 confirms the characteristic absorption bands of PLA, indicating its presence in the composite material. A strong peak at  $1753\text{ cm}^{-1}$  is attributed to the stretching vibrations of the C=O bond found in carboxylic or ester functional groups. This observation is reinforced by intense absorption bands in the  $1100\text{-}1200\text{ cm}^{-1}$  range, which are characteristic of the stretching vibrations of the C-O bonds in carboxylic acids and esters. Additionally, specific to PLA, the presence of saturated linear structures, particularly the  $-\text{CH}_3$  asymmetric and  $-\text{CH}_3$  symmetric types, is indicated by a weak band at  $2947\text{ cm}^{-1}$ . The bending frequencies for the  $-\text{CH}_3$  asymmetric and  $-\text{CH}_3$  symmetric groups have been identified at  $1446$  and  $1369\text{ cm}^{-1}$ , respectively [30-32] The incorporation of diacetin notably enhances the absorption band observed at  $1741\text{ cm}^{-1}$ . This enhancement can be attributed to the supplementary contributions from distinct carbonyl functional groups present within the molecular structure.

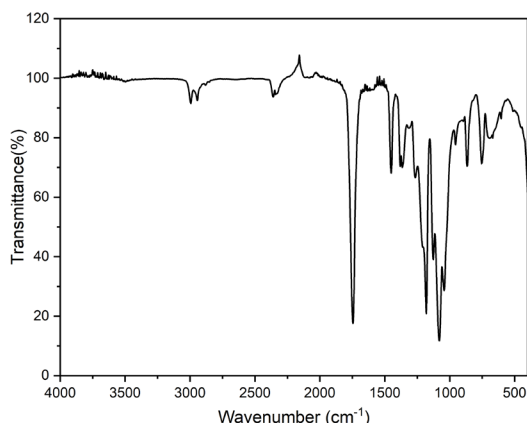


**Figure 3.** FTIR spectrum of sample PB2

The FTIR spectrum analysis, following the addition of oregano oil, reveals a peak at  $858\text{ cm}^{-1}$ . This peak can be attributed to the C–H out-of-plane bending associated with the structure of  $\beta$ -caryophyllene, a natural compound belonging to the sesquiterpene class known for its antibacterial and anti-inflammatory properties [33-35].

### Thermal properties

The thermogravimetric analysis (TGA) reveals a clear sequence of mass loss events, as shown in Figure 4, characteristic of the thermal behavior of the analyzed material. In the temperature range of 20–120 °C, the mass losses are negligible, indicating a low residual moisture content and good thermal stability in this lower region. A slight increase in mass loss is observed between 120–280 °C, which is attributed to the volatilization of low molecular weight organic compounds, such as oregano oil and the diacetin-type plasticizer. These compounds are not strongly bound within the polymeric matrix and are gradually eliminated through evaporation. The most significant mass loss, approximately 70%, occurs in the range of 280–350 °C and corresponds to the thermal degradation of polylactic acid (PLA). During this stage, chain scission and thermal decomposition of the base polymer take place, reflecting the thermal stability limits of the polymeric matrix under elevated temperature conditions.

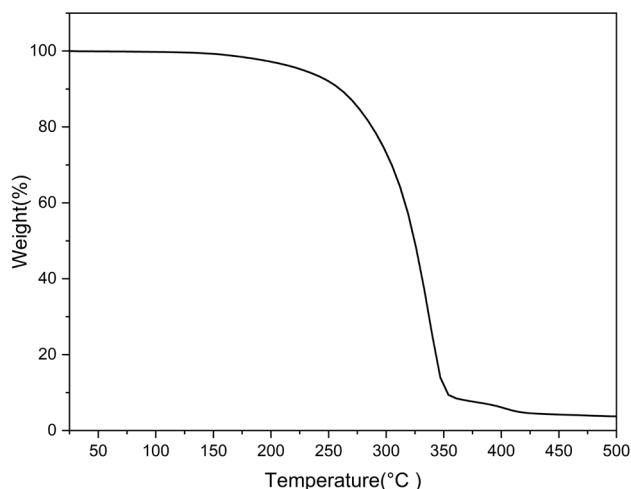


**Figure 4.** TGA curve of sample PB2

The effect of bioglass on the thermal transitions of PB2 sample composites is shown in the DSC thermogram (Figure 5). As can be seen, the addition of bioglass to PLA has a positive effect on the T<sub>g</sub> temperature, increasing it to above 83 °C. This behavior is attributed to the hindered mobility of the PLA segment due to the addition of bioglass which stiffens the PLA and delays the glass transition. The sample showed two endothermic peaks at 175 and 317 °C, probably caused by the melting of the amorphous structures, the size of the peaks being proportional to their concentration.

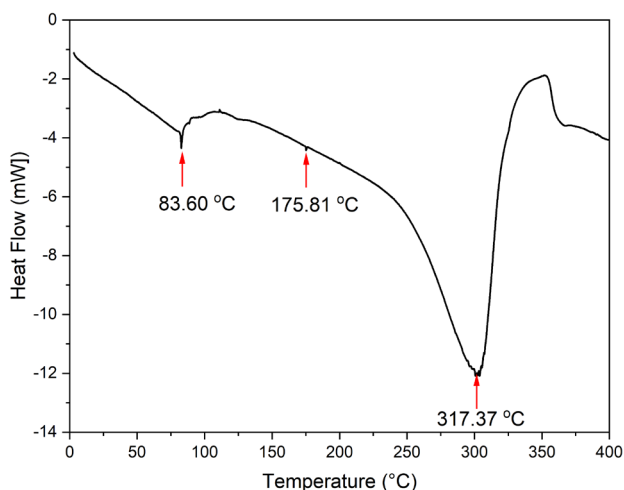


**Figure 5.** DSC thermogram of sample PB2

### Surface analysis

Scanning electron microscopy (SEM) analysis of the bioglass-reinforced PLA-Oregano oil (2%) film (PB2), shown at different magnifications (10  $\mu\text{m}$ , 50  $\mu\text{m}$ , and 200  $\mu\text{m}$ ) in Figure 6, reveals important insights into the morphology and dispersion behavior of the composite system. The relatively uniform distribution of bioglass particles throughout the polymer matrix indicates an effective dispersion, which is likely facilitated by the chemical compatibility between the diacetin plasticizer and the bioglass surface. This compatibility attributed to their close polarity enhances interfacial interactions, thereby promoting the formation of a more homogeneous and cohesive polymeric structure. Despite the generally smooth surface morphology observed across all magnifications, the presence of localized micro-aggregates of bioglass is evident, especially at higher resolutions. These micro-clusters

may result from areas with a locally insufficient concentration of diacetin, which limits its plasticizing and dispersive effect. Such aggregates, although minor, suggest that further optimization of the bioglass-to-diacetin ratio could improve the uniformity of dispersion and the overall microstructural integrity of the composite film. Overall, the SEM micrographs support the conclusion that the incorporation of bioglass into the PLA matrix was successful and reasonably well-distributed, with minimal surface defects, making the material potentially suitable for packaging applications.

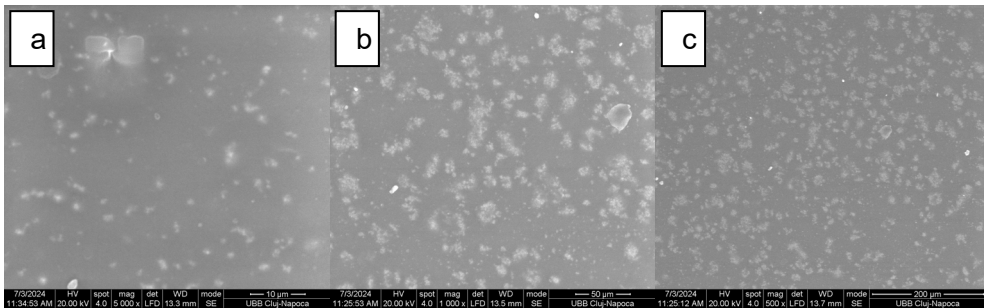


**Figure 6.** SEM micrographs of the PB2 sample reinforced with bioglass at different magnifications: (a) 10  $\mu\text{m}$ , (b) 50  $\mu\text{m}$ , and (c) 200  $\mu\text{m}$

Analysis of the PLA film surface by atomic force microscopy (AFM) provided a more detailed image of the microstructural units and topographic features, highlighting an advanced dispersion of bioglass nanoparticles as well as variations in the film thickness (Figure 7). The topographic image reveals uniformly distributed clusters of bioglass, suggesting good compatibility between the filler and the PLA matrix, This arrangement is caused by the composite flow during molding [36]. From the three-dimensional surface profile, a relatively homogeneous texture with similar topographic irregularities is observed. The calculated surface roughness parameters an average roughness (Ra) of 30.1 nm and a root mean square roughness (Rq) of 39.9 nm indicate a low to moderate roughness level, which may contribute positively to interfacial interactions in biomedical or dermato-cosmetic applications. These results confirm the successful incorporation of bioglass into the PLA matrix and support the morphological stability and uniformity of the composite surface.

THE INFLUENCE OF SOME POWDERS ON THE ANTIMICROBIAL ACTIVITY OF  
PLA PACKAGING WITH OREGANO OIL ADDITIVES

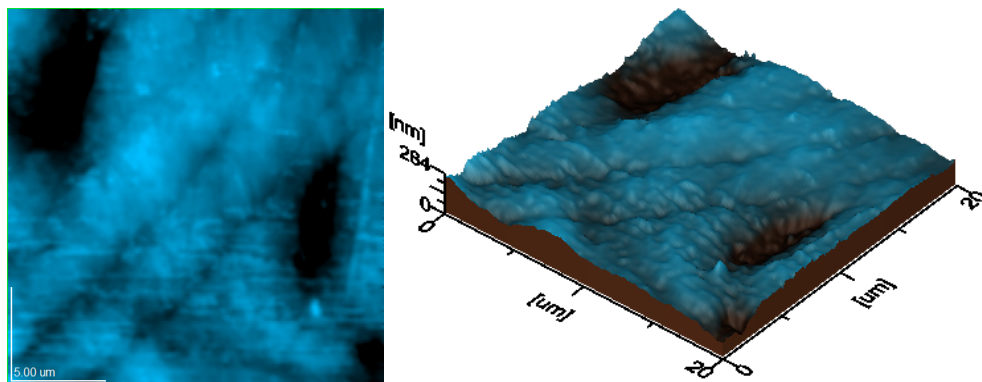


**Figure 7.** Topographic characteristics of the PB2 sample (a) topographic image; 3D image (scanned area 20 µm x 20 µm, Ra area 30.1 nm; Rq area 39.9 nm)

### Tensile test results

The mechanical performance of the bioglass-reinforced PLA composite containing oregano oil, plasticized with diacetin (PB2), reveals a noticeable alteration in tensile behavior compared to neat PLA. As shown in Table 1, the sample exhibited a maximum tensile strength of 25.91 MPa, with a maximum load of 305.39 N, and an elongation at break of 61.08 mm, while the Young's modulus was 2118.48 MPa. The stress at yield was recorded at 4.87 MPa.

**Table 1.** Mechanical parameters obtained from the tensile test of the PB2

Tensile strength (MPa)	Maximum load (N)	Elongation at break (mm)	Young's modulus (MPa)	Stress at yield (MPa)	Tensile strength (MPa)
25.912	305.3945	61.079	4.871	2118.479	5.182

Figure 8 illustrates the stress–strain curve, highlighting the characteristic deformation profile of the material. A distinct yield point is followed by a plastic deformation region, indicating ductile behavior prior to final rupture. The decrease in tensile strength and modulus, when compared to pure PLA, reflects a reduction in rigidity and load-bearing capacity. This can be attributed to the action of the diacetin-type plasticizer, which disrupts the crystalline domains of PLA and promotes the formation of a more amorphous structure. In turn, this facilitates chain mobility and leads to a marked increase in elongation

at break, enhancing the flexibility of the material. Such modifications confirm the role of diacetin in softening the PLA matrix and enabling better energy dissipation under stress, albeit at the expense of reduced mechanical strength. These properties may be favorable for applications requiring enhanced ductility and toughness, such as packaging applications.

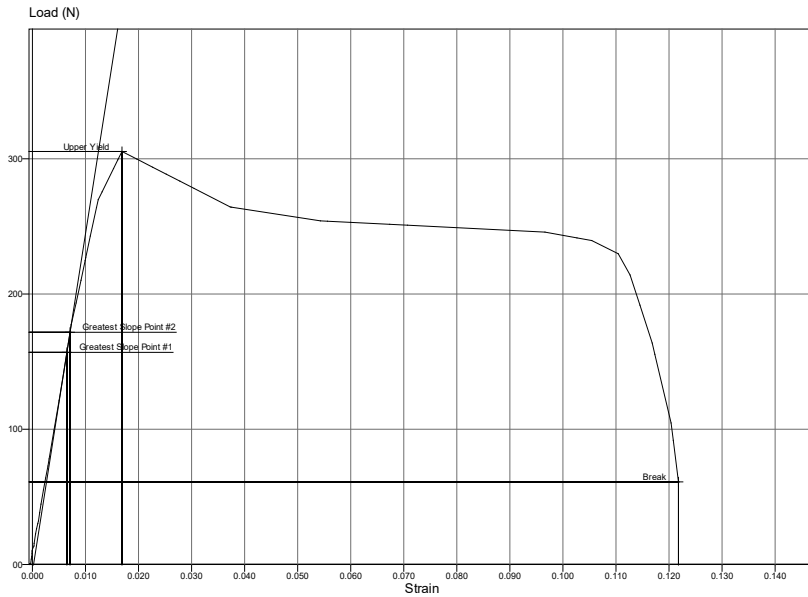


**Figure 8.** Stress–Strain Curve of PB2 sample

## CONCLUSIONS

The research aimed to evaluate the influence of some powders, such as activated carbon, aerosilica and bioglass, on the bactericidal efficiency of PLA-based food packaging plasticized with diacetins and added with oregano oil. The effectiveness over time of bactericidal compounds such as oregano oil can be improved by controlled release from the powders present in the composition of the active food packaging. Thus, in the first part of the research, the oregano oil content of the PLA films was optimized to ensure their efficient bactericidal activity. The optimization of the type of powder and the powder content of the composite were evaluated through microbiological

studies. Following these studies, a bactericidal activity of oregano oil in the presence of bioglass at a concentration of 3% was highlighted. In the second part of the study, the thermal and mechanical characteristics of the PLA composite based on bioglass plasticized with diacetins and added with oregano oil were determined. Experimental data revealed the decrease in mechanical properties of PLA and the improvement of elongation after plasticization with diacetin of PLA composite. Also, the T<sub>g</sub> temperature increased and surface examination indicated the presence of smooth samples with small micro-clusters of bioglass aggregates.

## **EXPERIMENTAL SECTION**

### **Materials and Methods**

Polylactic acid (PLA, Ingeo® brand, NatureWorks LLC, Tokyo, Japan), diacetin (used as a plasticizer, purchased from Sigma-Aldrich), and oregano essential oil (sourced from a local natural products supplier) were utilized for the preparation of biodegradable films. The components were dissolved in chloroform under constant stirring at 60 rpm and 50 °C for 30 minutes to ensure homogeneity. After complete solubilization, different powders activated carbon (Merck), Aerosil® 200 (Evonik Operations GmbH), or Bioglass® powder (NovaMin, Schott, USA) were incorporated into the polymer solution.

### **Preparation of food packaging films**

The solubilization process of polylactic acid (PLA) was carried out at a controlled temperature of 50 °C for 1 hour, using a stirring speed of 1400 rpm. Once complete dissolution of the PLA was achieved, the remaining components of each formulation were sequentially added to the solution. The resulting homogeneous mixture was then cast into sterile Petri dishes for film formation via solvent evaporation.

Three active food packaging formulations based on PLA were prepared, as summarized in Table 2. From each of the three films designated PD1, PD2, and PD3 twenty identical circular samples (disc-shaped) were punched, each with a diameter of 7 mm. These test specimens were individually transferred into sterile, sealed vials to prevent external humidity and preserve their structural and microbial integrity prior to testing.

**Table 2.** Composition of PLA-based film formulations

Sample	PLA (% w/w)	Diacetin (% w/w)	Powder (type and % w/w)	Oregano oil (% w/w)
PD1	74.0	25	–	1.0
PD2	73.5	25	–	1.5
PD3	73.0	25	–	2.0
PC1	71.0	25	Activated carbon: 2.0	2.0
PC2	70.0	25	Activated carbon: 3.0	2.0
PS1	71.0	25	Aerosil 200: 2.0	2.0
PS2	70.0	25	Aerosil 200: 3.0	2.0
PB1	71.0	25	Bioglass: 2.0	2.0
PB2	70.0	25	Bioglass: 3.0	2.0

### Biological Culture Preparation and Microbiological Setup

The biological materials used in this study included *Bacillus subtilis* bacterial cultures and *Chlorella* sp. algal cultures, both of which were supplied by the Microbiological Studies Laboratory at the Petroleum-Gas University of Ploiești, Romania [37]. All microbiological tests were conducted in accordance with the OECD Guidelines for the Testing of Chemicals issued by the Organisation for Economic Co-operation and Development (OECD), and in compliance with the standards outlined in USP 35-NF 30 (Pharmacopeial Convention): Microbiological Enumeration of Non-Sterile Products – Tests for Specified Microorganisms.

To support experimental determinations, several analytical instruments were employed. Monitoring of microbial viability during the test period was conducted using a CELESTRON digital microscope, model 4434. Gravimetric measurements were performed using an OHAUS analytical balance, model AX224M. Physicochemical parameters of the culture media such as pH, conductivity, and dissolved oxygen content were recorded using a WTW Inolab Multi 9630 IDS multiparameter meter. This advanced instrument features three galvanically isolated measurement channels, enabling simultaneous and accurate tracking of all relevant parameters critical for evaluating biological responses.

The biological materials used in this study included *Bacillus subtilis* bacterial cultures and *Chlorella* sp. algal cultures, both of which were supplied by the Microbiological Studies Laboratory at the Petroleum-Gas University of Ploiești, Romania [26]. All microbiological tests were conducted in accordance with the OECD Guidelines for the Testing of Chemicals issued by the Organisation for Economic Co-operation and Development (OECD), and in compliance with the standards outlined in USP 35-NF 30 (Pharmacopeial

Convention): Microbiological Enumeration of Non-Sterile Products – Tests for Specified Microorganisms.

To support experimental determinations, several analytical instruments were employed. Monitoring of microbial viability during the test period was conducted using a CELESTRON digital microscope, model 4434. Gravimetric measurements were performed using an OHAUS analytical balance, model AX224M. Physicochemical parameters of the culture media such as pH, conductivity, and dissolved oxygen content were recorded using a WTW Inolab Multi 9630 IDS multiparameter meter. This advanced instrument features three galvanically isolated measurement channels, enabling simultaneous and accurate tracking of all relevant parameters critical for evaluating biological responses.

To evaluate the antimicrobial and algal inhibitory activity of the PLA-based films, two specific growth media were prepared: one for bacterial cultivation and one for algal propagation.

The bacterial growth medium (MB) was composed of: bacto-peptone (10 g), sodium chloride (5 g), agar (20 g), meat extract (10 g), and distilled water up to 1000 mL. The pH was adjusted to 7.5.

The algal growth medium (MA) contained: agar (20 g), magnesium sulfate heptahydrate ( $\text{MgSO}_4 \cdot 7\text{H}_2\text{O}$ , 1.2 g), potassium nitrate ( $\text{KNO}_3$ , 1.2 g), calcium chloride ( $\text{CaCl}_2$ , 1.6 g), sodium phosphate monobasic dihydrate ( $\text{NaH}_2\text{PO}_4 \cdot 2\text{H}_2\text{O}$ , 1.2 g), ferrous sulfate heptahydrate ( $\text{FeSO}_4 \cdot 7\text{H}_2\text{O}$ , 0.08 g), sodium nitrate ( $\text{NaNO}_3$ , 1.2 g), and ammonium chloride ( $\text{NH}_4\text{Cl}$ , 0.8 g), dissolved in distilled water to 1000 mL. The pH was adjusted to 6.5.

Both media types were sterilized in an autoclave at 121 °C for 15 minutes prior to inoculation and pouring.

Following sterilization, the media were poured into sterile Petri dishes in two parallel experimental series:

Series A – targeting bacterial growth promotion (*Bacillus subtilis*)

Series B – targeting algal growth promotion (*Chlorella* sp.)

Each experimental series was tested on three types of PLA-based films (PD1, PD2, and PD3), and each sample was evaluated in triplicate.

For Series A, nine Petri dishes were filled with 25 mL of MB medium cooled to approximately 40 °C and inoculated with 2 mL of *Bacillus subtilis* bacterial suspension at a concentration of  $10^{-4}$  cells/mL. After solidification, the plates were labeled 1–9 (Figure 9).

Plates 1–3 received five circular film samples from PD1

Plates 4–6 received five discs from PD2

Plates 7–9 were loaded with PD3 samples

All dishes were sealed and incubated at 30 °C for 14 days to monitor bacterial growth or inhibition zones.

For Series B, the same protocol was applied, except that the MA medium (algal-specific) was used and the plates were inoculated with *Chlorella* sp. cultures at the same concentration ( $10^{-4}$  cells/mL). As with the bacterial series, nine Petri dishes were used to evaluate the three film types in triplicate (PD1, PD2, PD3). These plates were maintained at 24 °C under controlled light conditions using a 12-hour light/dark photoperiod to simulate natural algal growth conditions.

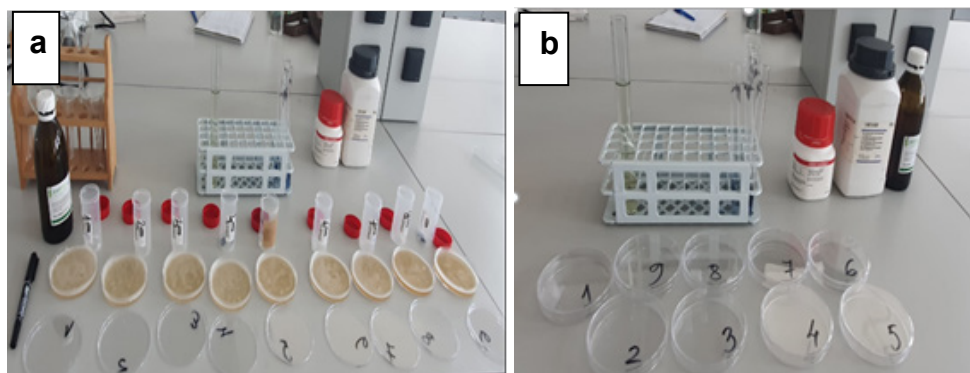


**Figure 9.** Workflow representation of the experimental stages for the evaluation of PD1, PD2, and PD3 films in the MB series: (a) Arrangement of perforated PLA film discs (7 mm diameter) into groups according to sample type (PD1, PD2, PD3); (b) Labeling of sterile Petri dishes containing MB culture media inoculated with *Bacillus subtilis* for microbiological testing

### Characterization of PLA-Based Food Packaging Films

To gain a comprehensive understanding of the physicochemical and mechanical behavior of the developed PLA-based composite films, a series of structural, thermal, mechanical, and surface analyses were carried out using state-of-the-art techniques. These characterizations aimed to evaluate the impact of active additives such as Bioglass®, oregano oil, and various powders on the overall performance and functionality of the films.

Fourier Transform Infrared Spectroscopy (FTIR): was employed to investigate the molecular structure and the specific functional groups present in the PLA matrix and its composite formulations. The analysis was conducted using a Shimadzu IRTracer-100 spectrometer (Kyoto, Japan), operating in the  $4000\text{--}500\text{ cm}^{-1}$  spectral range with a resolution of  $4\text{ cm}^{-1}$ . The recorded spectra revealed characteristic absorption bands associated with the PLA backbone as well as distinct peaks indicating the successful incorporation of bioactive and inorganic additives.

**Thermal Properties Analysis (TGA/DSC):** The thermal behavior and stability of the PLA–Bioglass® composites were assessed via thermogravimetric analysis (TGA) and differential scanning calorimetry (DSC). TGA and DTG measurements were performed using the TGA 2 Star System (Mettler Toledo, Zurich, Switzerland) under a nitrogen atmosphere, with a temperature ramp from 25 °C to 500 °C at a controlled rate of 5 °C/min. These analyses provided detailed insights into thermal degradation patterns and mass loss events.

Complementary DSC measurements were carried out using a DSC 3+ Star System (Mettler Toledo, Leicester, UK), under nitrogen, with a heating rate of 10 °C/min across a range of 25–400 °C. The thermal transitions including glass transition temperature ( $T_g$ ), crystallization, and melting points were evaluated to determine the influence of bioglass and essential oil components on the thermal profile and phase behavior of the PLA matrix.

The mechanical performance of the composite films was investigated using a Lloyds Instron Universal Testing Machine (Lloyd Instruments, AmetekIns, West Sussex, UK), controlled by Nexygen software version 4.0. Tensile tests followed the EN ISO 527-3:201 standard and were performed on rectangular film specimens measuring 3 mm in thickness, 4 mm in width, and 40 mm in length, with a calibrated gauge area of 25 × 25 mm. A constant axial force of 5 N was applied at ambient temperature until sample failure. From the resulting stress–strain curves, key mechanical parameters were extracted, including: Ultimate Tensile Strength (UTS), Elongation at Break ( $\epsilon$ ), Young’s Modulus (E). These parameters provided critical information regarding the tensile behavior, ductility, and stiffness of the different formulations, directly influencing their suitability for food packaging applications.

**Surface Morphology and Microstructural Analysis:** The surface features and microstructure of the PLA composites were examined using high-resolution imaging techniques, including scanning electron microscopy (SEM) and atomic force microscopy (AFM) [38]. SEM images were acquired using an Inspect™ microscope (FEI, Hillsboro, OR, USA) operated under high vacuum at an accelerating voltage of 30 kV. This method enabled detailed visualization of the dispersion of fillers, phase separation, and surface homogeneity. AFM investigations were carried out using a JEOL JSPM-4210 instrument (JEOL, Tokyo, Japan), scanning a surface area of 20  $\mu\text{m}$  × 20  $\mu\text{m}$ . The resulting three-dimensional surface maps were analyzed with JEOL WIN SPM 2.0 software to assess nanoscale roughness, uniformity, and potential interactions between the polymer matrix and the incorporated additives. Together, SEM and AFM analyses provided complementary insights into the morphological and interfacial properties of the films.

**Acknowledgments:** “Development of innovative food packaging without negative impact on the environment (AMBAL-INOV)”, My SMIS: 120994, contract: 375/390051/30.09.2021, Competition: 63/POC/163/1/3/LDR.

## REFERENCES

1. Y. A. Hamdan; H. Oudadesse; S. Elouali; N. Eladlani; B. Lefeuvre; M. Rhazi; *International Journal of Biological Macromolecules*, **2024**, 278, 134909.
2. C. G. Gheorghe; O. Pantea; V. Matei; D. Bombos; A.C. Borcea; *Revista de Chimie*, 2011, 62, 707-711.
3. M. Ferdes; F. Al Juhaimi; M.M. Özcan; K. Ghafoor; *South African Journal of Botany* **2017**, 113, 457-460.
4. T. Marino; E. Blasi; S. Tornaghi; E. Di Nicolò; A. Figoli; *Journal of Membrane Science*, **2018**, 549, 192-204.
5. C. G. Gheorghe; O. Pantea; V. Matei; D. Bombos, A. C. Borcea; *Revista de Chimie*, **2011**, 62, 926-929.
6. M.A. Elsayy; K.H. Kim; J.W. Park; A. Deep; *Renewable and Sustainable Energy Reviews*, **2017**, 79, 1346-1352.
7. T.A. Otitoju; C. H. Kim; M. Ryu; J. Par; T. K. Kim; Y. Yoo; H. Park; J.H. Lee; Y.H. Cho; *Journal of Cleaner Production*, **2024**, 467, 142905.
8. C. G. Gheorghe, C; O. Pantea; V. Matei; D. Bombos; A. F. Borcea; *Revista de Chimie*, **2011**, 62, 1023-1026.
9. S.A. Varghese; S. Siengchin; J. Parameswaranpillai; *Food Bioscience*, **2020**, 38, 100785.
10. T. R. Putri; A. Adhitasari; V. Paramita; M. E. Yulianto, H.D. Ariyanto; *Materials Today: Proceedings*, **2023**, 87, 192-199.
11. H.C. dos Santos; B. E. Stutz; A.F. Young; *Renewable Energy*, **2024**, 237, 121943.
12. C. G. Gheorghe; O. Pantea; V. Matei; D. Bombos; A.C. Borcea; *Revista de Chimie*; **2011**, 62, 582-584.
13. M. Johar; A. Rusli; *Materials Today: Proceedings*; **2022**, 66, 2957-2961.
14. A.K. Tyagi; A. Malik; *International Journal of Food Microbiology*; **2010**, 143, 205-210.
15. D.R. Popovici; C. G. Gheorghe; C.M. Dușescu-Vasile; *Bioengineering*; **2024**, 11, 1306.
16. K. Abouelezz; M. Abou-Hadied; J. Yuan; A. A. Elokil; G. Wang; S. Wang; Wang; G. Bian; *Animal*; **2019**, 13, 2216-2222.
17. L. Krishnan; P. Chakrabarty; K. Govarthan; S. Rao; T.S; *International Journal of Biological Macromolecules*; **2024**, 277, 133073.
18. V Gheorghe; C.G. Gheorghe; A. Bondarev; V. Matei; M. Bombos; *Revista de Chimie*; **2019**, 70, 2996-2999.

THE INFLUENCE OF SOME POWDERS ON THE ANTIMICROBIAL ACTIVITY OF  
PLA PACKAGING WITH OREGANO OIL ADDITIVES

19. N. M. Nasir; A. Jusoh; H. Manan; N.A. Kasan; A. S. Kamaruzzan; W. A. W. A. K. Ghani; S. B. Kurniawan; F. Lananan; *Biocatalysis and Agricultural Biotechnology*; **2023**, *47*, 102596.
20. Y. Su; Z. Cheng; Y. Hou; S. Lin; L. Gao; Z. Wang; R. Bao; L. Peng; *Aquatic Toxicology*; **2022**, *244*, 106097.
21. P. Parmar; R. Kumar; Y. Neha; V. Srivatsan; *Frontiers in Plant Science*; **2023**, *14*, 1073546.
22. C. G. Gheorghe, C. Dutescu; M. Carbureanu; *Revista de Chimie*; **2016**, *67*, 2106-2110.
23. G. M. Vingiani; P. De Luca; A. Ianora; A.D.W. Dobson; C. Lauritano; *Marine Drugs*; **2019**, *17*, 459.
24. A. A. Singh; S. Sharma; M. Srivastava; A. Majumdar; *International Journal of Biological Macromolecules*; **2020**, *153*, 1165-1175.
25. OECD. Test No. 201: Freshwater Alga and Cyanobacteria, Growth Inhibition Test, OECD Guidelines for the Testing of Chemicals, Section 2. 2011.
26. M. Roszak; J. Jabłońska; X. Stachurska; K. Dubrowska; J. Kajdanowicz; M. Gołębiewska; A. Kiepas-Kokot; B. Osińska; A. Augustyniak; J. Karakulka; *International Journal of Molecular Sciences*; **2021**, *22*, 13469.
27. A. Silva; S. A. Figueiredo; M.G. Sales; C. Delerue-Matos; *Journal of Hazardous Materials*; **2009**, *167*, 179-185.
28. C. G. Gheorghe; C. M. Dutescu-Vasile; D. R. Popovici; D. Bombos; R. E. Dragomir; F. M. Dima; M. Bajan; G. Vasilievici; *Toxics*; **2025**, *13*, 368.;
29. V. Gheorghe; C. G. Gheorghe; D. R. Popovici; S. Mihai; R. E. Dragomir; R. Somoghi; *Bioengineering*; **2024**, *11*, 623.
30. C.-S. Wu.; H.-T. Liao; *Polymer*; **2005**, *46*, 10017.
31. B.W. Chieng; N.A. Ibrahim; W.M. Yunus; M.Z. Hussein; *Polymers*; **2014**, *6*, 93
32. P. Singla; M. Rajeev; B. Dusan; S.N. Upadhyay; *Journal of Macromolecular Science*; **2012**, *49*, 963
33. C. Kamaraj; G. Balasubramani; C. Siva; M. Raja; V. Balasubramanian; R.K. Raja; S. Tamilselvan; G. Benelli; P. Perumal; *Journal of Cluster Science*; **2017**, *28*, 1667
34. D. Vârban; M. Zăhan; I. Crișan; C.R. Pop; E. Gál; R. Ștefan; AM. Rotar; A.S. Muscă; S.D. Meseșan; V. Horga; I. Lados; O. Loredana; A. Stoie; R. Vârban; *Plants*, **2023**, *12*, 4017.
35. F. Francomano; A. Caruso; A. Barbarossa; A. Fazio; C. La. Torre; j. Ceramella; R. Mallamaci; C. Saturnino; D. Iacopetta; M.S. Sinicropi; *Applied Sciences*; **2019**, *9*, 5420.
36. A. Moldovan, S Cuc, D. Prodan, M. Rusu, D. Popa, I. Petean, D. Bomboș; O. Nemes; *Polymers*; **2023** *15*, 2855.
37. V. Gheorghe; C. G. Gheorghe; A. Bondarev; R. Somoghi; *Toxics*; **2023**, *11*, 285.
38. A. Moldovan; I. Sarosi; S. Cuc; D. Prodan; A.C. Taut; I. Petean; D. Bombos; R. Doukeh; S.C. Man; *Journal of Thermal Analysis and Calorimetry*; **2024**, *150*, 2469–2481.

